Synchronisation Control Action for Very Low-Frequency Oscillations

Synchronisation Control Action for Very Low-Frequency Oscillations

Connor Duggan, Paul Brogan, Xueqin Liu, Robert Best and John Morrow
School of Electronics, Electrical Engineering and Computer Science
Queen's University Belfast
Belfast, United Kingdom

***Abstract*—Very low-frequency oscillations have been occurring on power grids with a high concentration of hydro generation and islanded grids with a lack of AC interconnection. These oscillations can persist in an ambient form or be triggered by a transient event before growing to the extent that threatens system stability. When a severe event occurs, it is important to identify the cause and have practical control actions to restore power system stability. Firstly, this paper demonstrates that synchronising a generator with a positive damping torque component can restore positively damped conditions. Simulations on a modified 2-Area system are evaluated with DIgSILENT PowerFactory. A transport delay is added to speed feedback of a GAST model governor to simulate a spontaneous negatively damped very-low-frequency oscillation with the appearance of being self-excited after a generation load imbalance. Secondly, a 300 mHz 0.08 Hz very-low-frequency oscillation on the Irish electrical grid is analysed using the governor based distributed energy flow method. Dissipating energy flow is used to illustrate how the synchronisation of 2 generators successfully returned the Irish power system to positively damped conditions.**

Keywords- Very Low-Frequency Oscillations, DEF, Control Decisions, wide-area monitoring and control, power system stability

I. INTRODUCTION

A. Motivation

Low damped power system oscillations and poor frequency regulation decrease power system stability and increases wear and tear on devices connected to the power system [1], [2]. Very low-frequency oscillations (VLFOs) are a class connected to a taxonomy of power system oscillations, characterised by an oscillation frequency between 0.001-0.16 Hz and phase differences tenths of degrees observed in synchrophasors located across the power system.

A decrease in VLF mode damping is primarily attributed to negatively damped governors [3]. To date, the majority of VLFO research relates to hydro generation where they arise due to the time delay related to the water hammer time constant [4]. VLFOs have occurred on hydro dominated systems such as Yunnan [5], Canada [6] and Colombia [7]. VLFOs are also arising on power systems with a low concentration of hydropower, such as Ireland[8]–[10] , Great Britain [11] and Australia [12]. VLFOs have been investigated by Ireland's TSO, concluding that the occurrence of events cannot be linked to any system level measure such as System Non-Synchronous Penetration (SNSP), wind penetration or inertia [8]. A correlation was found where VLF events tended to occur when the nominal system frequency was above 50 Hz, and inertia was low.

B. Literature Review

Historically, oscillation studies focused on electromechanical oscillations that occur at frequencies greater than 0.1Hz. Electromechanical oscillations are often attributed to high power transfers and rotor angle interactions excited by random load movements or short circuits. Whereas VLFOs are strongly linked to governor control settings. RMS Energy Filter, mode shape [11], and Dissipating Energy Flow (DEF)[13], [14] [15] are three successful methods for locating VLFOs that are widely used in literature. The method in [16] filters a chosen PMU measurement, usually voltage magnitude or active power. It calculates the signal energy at the frequency bands associated with VLF, inter-area, local and torsional modes.

VLF mode shape analysis is presented in [11], where the authors indicate that the leading phase of the oscillation is the source. This interpretation is also consistent with electromechanical mode shape theory [17]. Reference [11] also indicates wind generation may be a VLFO source under certain conditions. DEF is a proven technique for locating natural and forced oscillations [15] and has successfully located over 1200+ events for ISO New England [18].

Modelling VLFOs for simulation-based studies, small signal stability analysis [3] and time-domain non-linear analysis [19] are commonly used. Reference [20] used a transport delay for simulating oscillations on a steam-based governor but for oscillation frequencies greater than 0.1 Hz. *Flynn et al* [21] express boiler control systems on steam turbines could have long delays within their subsystems that can make control challenging, possibly causing a divergence from the linear relationship of droop control.

Several mitigation techniques have been proposed within literature to increase the damping of the VLF mode. [21] proposed tuning PI parameters to increase the damping of a governor control system. Optimised Multi-Band Power System Stabilisers (MBPSS) can improve the damping ratio of the VLF mode [22], [23]. Converter Interfaced Generation (CIG) such as BESS [24] and type-3-windfarms [25] can increase the damping of VLFOs by providing active power out of phase with the measured local frequency deviation.

A real-time suppression strategy has been proposed in [14], which shows in simulation-based studies that turning off the governor will increase the damping ratio by providing the dominant-negative damping component. In Ireland [8], the real-time activation of Active Power Control (APC) at wind farms has proved an effective means to increase the VLF mode's damping ratio instantaneously.

C. Contributions

Contributions of this paper include:

- Impact of a transport delay on speed-feedback of a GAST [26] governor model. The oscillation frequency and damping ratio of the VLF mode will be compared for transport delays between 1 and 6 seconds.
- The impact of synchronising two generators on the damping ratio during a poorly damped VLF event
- A significant VLFO on the Irish power system is analysed with DEF providing pre-event, during event and post-event results.

II. Methodology

A. Characteristics of VLFOs

During VLFOs, synchronous generators oscillate with approximately coherent phase in observed frequency measurements [27], as shown in Fig 1. It has been proposed in [28] that a VLFO can be modelled using a single frequency assumption where all generation and load sources can model as a global swing equation.

$$\frac{d\omega}{dt} = \frac{\Delta P}{2H} = \frac{\sum P_m - \sum P_e}{2H} \quad (1)$$

Where ω is system speed, H is the inertial constant under a single frequency assumption, ΔP is an active power imbalance, P_m is mechanical power and P_e is electromagnetic power. Equation 1 defines the coherent mode shape that is commonly observed. The sub axis in Fig. 1 (a) shows a zoomed-in plot of frequency measurements across 4 different geographical locations during the event. The small relative phase difference between different geographical locations is a characteristic of VLFOS. Fig 1. represents the VLFO analysed in this paper. The Irish system's VLF mode has a highly mobile oscillation frequency and amplitude during sensitised periods. It is not unusual for a sudden change in the VLF oscillation mode due to what appears to be a self-excited governor. Fig 1. presents an example of this phenomenon where a poorly damped oscillation of approximately 40mHz was observed before the event, with an oscillatory mode of 0.06Hz. However, after the 100 s mark, the oscillation mode changed to 0.08 Hz and became negatively damped a short time after. This self-exciting mode is likely due to a delay time within governor controls, where the time value determines the frequency of oscillation.

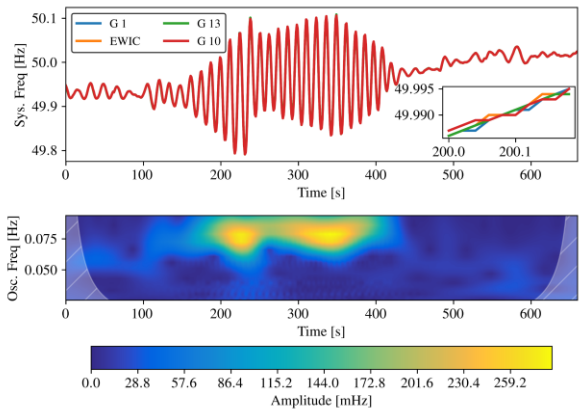

Fig. 1: a. System Frequency of 300 mHz peak-peak oscillation with subplot representing the coherent mode shape b. Continuous Wavelet Transform (CWT) of system frequency in shown in plot (a)

B. Transport Delay within Governor Control System

Control valves within a gas or steam turbine will modify the injection of liquid fuel or steam. Control valves will also possess non-linear flow characteristics such as backlash. This non-linearity can cause a divergence from the linear relationship from the droop control within a governor control system. Fig 2 shows the frequency regulation process with a generic transport delay added to the governor's speed feedback. Transport delay within the control loops will affect the control valves' ability to recognise the input change and make an effective correction. This paper will model this phenomenon using a generic transport delay within the governor's speed input. The controller will signify the control valve after the transport delay time set. This deadtime accounts for the load changes that remain undetected, creating oscillations and, consequently, inaccuracy between speed and the gate/valve position.

C. Governor Based DEF

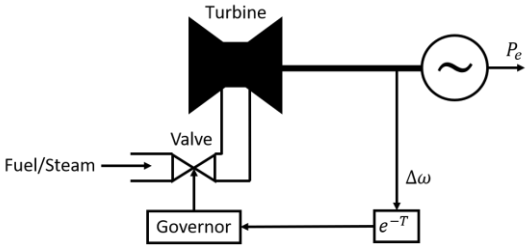

Fig 2: Simplified flow diagram of governor frequency regulation process with transport delay

Demonstrated in [14] is a modification of DEF to evaluate the damping response from a governor. Transient energy flow into the governor can be evaluated as

$$W_{pm}^{D} = \int -\Delta P_m d\Delta\delta = \int -\Delta P_m \omega_0 \Delta\omega dt \quad (2)$$

Where δ is the rotor angle, ω_0 synchronous angular velocity , ω is the generator speed and P_m is mechanical power. Since VLFOs have a coherent mode shape, the generator speed can be calculated from a PMU connected at the high voltage or low voltage side of the generator bus as:

$$\Delta\omega = \frac{\Delta f}{f_0} = \frac{f - f_0}{f_0} = \frac{d\theta}{f_0} \quad (3)$$

P_m can be subsequently evaluated as:

$$P_m = P_e + 2H\frac{d\Delta\omega}{dt} \quad (4)$$

P_e can be derived explicitly from PMU data and reasonable estimates are available for the inertial constant of synchronous machines (TSOs will have access to much more accurate values). The steps employed to process DEF in this investigation are similar to those employed in [14]. Analysis of the Irish system is complicated by the variability of the VLF mode frequency. Therefore, a zero-phase FIR bandpass

filter is employed with a passband of 0.01 to 0.12 Hz. It is important to note for DEF into the governor that the generator that produces positive damping has a positive cumulative sum, which is the opposite of the DEF method used commonly for forced and natural electromechanical oscillations [18].

III. VLFOs ON MODIFIED 2-AREA SYSTEM

This paper's simulations are evaluated on a modified 2-area test system in DIgSILENT PowerFactory shown in Fig 3. All generators are modelled using the GENROU model with the same synchronous machine characteristics. G1, G2, G3 and G4 have an MVA base of 900 and G5 and G6 have an MVA base of 100. The droop setting is set to 0.03 on G1 and G5-G6 and 0.05 on G2-G4. Parameters for the generators and loads can be found in Appendix A. A load is attached to bus nine, which will create a step response that excites the VLF mode through a generation load imbalance. No Automatic Voltage Regulators (AVRs) or Power System Stabilizers (PSS) are used in the simulations. Small signal

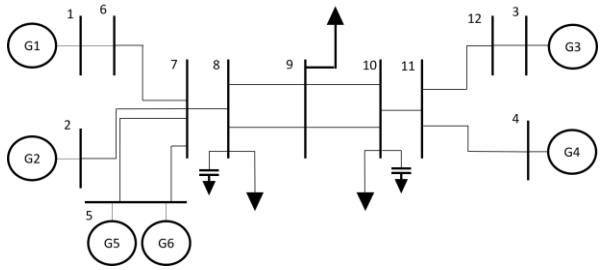

Fig 3: Modified Kundur 2 Area System

analysis indicates a VLF mode of 0.005 Hz. However, it does not have an observed coherent mode shape, so it is not considered a VLF mode.

A. Effect of Time Delay in Governor

A GAST governor with a speed deadband and generic transport delay is added to all six generators. The deadband is set to 0 for G1, G2, G3 and G4 to activate the governor and set to 1 in G5 and G6 to disable a governor response. A load event in PowerFactory is used with a proportional active power step change of 100000%. This load event will create a 10MW load step change at bus nine after 10 seconds. The transport delay is changed at G1 from 1 to 6 seconds in 0.5 increment steps before each simulation to create badly damped conditions. Although frequency and damping of the mode will depend on the time constants and gain within the GAST governor model, a variation of such governor parameters is not examined given this paper's constraints.

Table 1 shows the oscillation frequency and damping of the VLF mode calculated using the TLS-ESPRIT [29] algorithm. It shows that as the delay time increases from 1 second, the dominant oscillation mode frequency and damping decreases. Table 1 and Fig 4. (a) show that when there is a delay in the governor's speed feedback, this will decrease the VLF mode's damping ratio. The damping ratio is minimal with a delay of 2 seconds and gradually increases from a delay time of 2 seconds, and reaches positively damped conditions at approximately 5 seconds. The governor-based energy flow method was used when the time delay was equal to 3 in governor G1 is shown in Fig 4. (b). G1 is the oscillation source, with G2, G3 and G4 providing almost identical positive damping components. This is expected as identical governor parameters are used for G2-G4. Since G5-G6 have identical governor settings as G2-G4 apart from the droop response,

T [s]	f [Hz]	ζ [%]	T [s]	f [Hz]	ζ [%]
1	0.199	3.531	4	0.098	-0.579
1.5	0.173	-0.722	4.5	0.090	-0.242
2	0.151	-1.823	5	0.083	0.030
2.5	0.134	-1.797	5.5	0.077	0.249
3	0.120	-1.416	6	0.071	0.426
3.5	0.108	-0.979			

TABLE 1: Impact of delay time. T = Generic transport time delay, f and ζ oscillation frequency and damping respectively

G5 and G6 will provide and damping response when synchronised.

B. Synchronisation of G5 and G6

The governor response of G5 and G6 were disabled at the start of the simulation by setting the deadband parameter to 1. Governor control at G5 and G6 was activated by

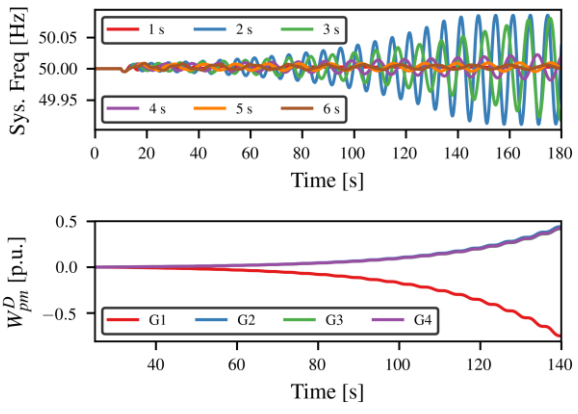

Fig 4: (a)Average system frequency for delay time 1,2,3,4,5 and 6 (b) W_{pm}^{D} when delay time of G1 is 3s

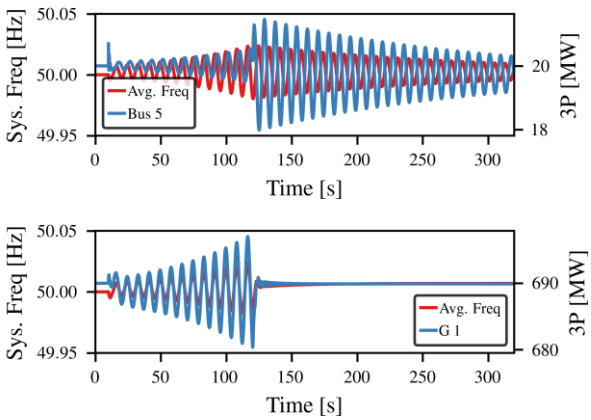

Fig 5: (a) Synchronization of G5 & G6 (b) Disabling governor control at G1

executing a parameter event at 120s by changing the deadband of G5 and G6 to 0. Activating governor response immediately to damp the VLFO and effectively synchronising the generator for VLFO damping can be observed in Fig 5. (a). The governors' activation immediately returns the system to positively damped conditions, and the VLFO decays gradually.

Although this simulation shows that synchronising governors with a positive damping torque component can return the system to positively damped conditions, there will be limitations on the start-up time. Large coal-fired and combined-cycle gas turbines (CCGTs) will not have this capability. Pumped storage and OCGT units on the Irish system have listed start-up times of six minutes but can be synchronised more quickly. Although G5 and G6 do return the system to positively damped conditions, Fig. 5 (b) shows that the most effective control action is to deactivate the governor at G1. Deactivating the governor removes the VLFO with immediate effect. This is considered a much more effective and cheaper solution for TSOs[7].

IV. Analysis of 300 Millihertz VLFO

A. Introduction

A VLF event occurred on the Irish system in 2018, displayed in Fig. 1 and Fig. 6. This case is of particular interest because no clear excitation event was observed, unlike previous severe Irish system cases. During this event, the two standalone grids that form the Irish power system were split for scheduled maintenance. The oscillations were only measured on the Republic of Ireland (ROI) system, as Fig. 6 shows. It is worth noting that a VLF mode was existent on the Northern Ireland (NI) system, but no significant VLFOs were observed.

ROI's power system was operating at a system demand of 2964 MW, wind penetration of 30%, exporting ~150 MW to GB through the east-west interconnector (EWIC), and synchronous based inertia was approximately 27,000 MWs. Ireland's grid code requirements dictate that all conventional dispatchable generation must have PFR (Primary Frequency Response) turned on [30]. APC was not activated pre-or post-event, and the EWIC interconnector did not provide frequency response according to PMU data.

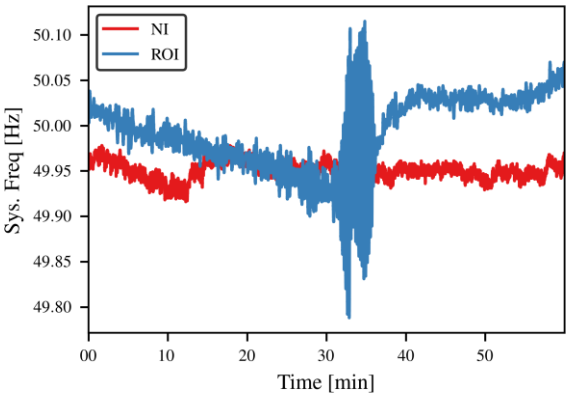

Fig 6: System Frequency for 300mHz event when NI and ROI where islanded

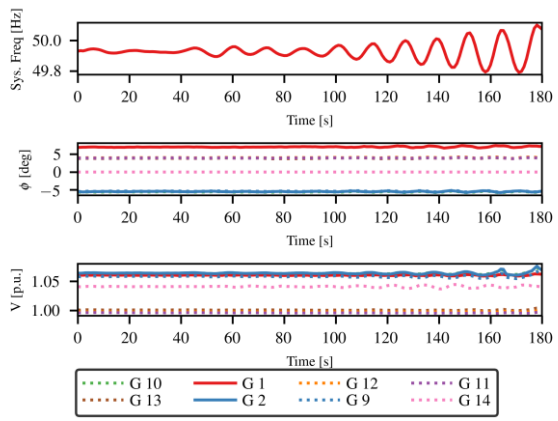

Fig 7: (a) System Frequency trace (b) Phase difference between generators where G14 as th reference (c) Line-line voltage magnitude

B. Evidence of Exciting Event

Fig 7 shows the system frequency trace, phase difference and voltage magnitude for the VLFO event. The VLFO was not preceded by a transient event, such as a short circuit or generator trip, as indicated by Fig. 7. It appears that the event is spontaneous, resulting from a governor self-exciting, like the time delay analysis in Section III A. The event has a natural mode shape, and no harmonics are observed, meaning it is doubtful that it is a forced oscillation.

The generator that caused the oscillation likely has a sizeable intentional delay in the governor control loop. While the delays may be added to reduce generator power swings and load cycles, they can create a backlash component and potentially self-exciting oscillations. For an oscillation event of this magnitude to occur, other synchronised generators synchronised must also be providing little or no damping and potentially negative damping of the VLF mode.

The conditions that led to this event may include,

- A self-exciting 0.08 Hz mode within a governor
- A loss of damping from governors in Northern Ireland

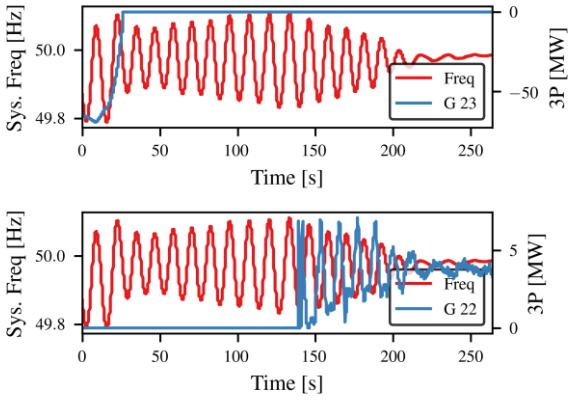

Fig 8: System Frequency for 300mHz event when NI and ROI where islanded

- A frequency deviation of –0.1 Hz with the change in mode amplitude and frequency when the frequency reached 49.9 Hz

C. Control Actions

Several control actions to mitigate the oscillation are evident in the PMU data. The first observed control action is shown in Fig.8(a), a pumped storage site that was pumping at the onset of the event is switched out of service, reducing load and raising system frequency closer to nominal. Since the oscillation began when ambient frequency oscillations clipped 49.9 Hz, bringing system frequency closer to 50 Hz may have reduced the gain in a self-exciting governor. The control operation on G23 markedly reduced the oscillation magnitude but did not change the mode's damping ratio. G23 did not participate in the oscillation, but desynchronising G23 did reduce the oscillation magnitude and buy the operator time for the two other governors' synchronisation.

The system returned to positively damped conditions after desynchronisation of G22. Another unit was synchronised, but unfortunately, it is not monitored through Ireland's PMU network. However, due to the machines being the same and belonging to the same power station, it can be assumed that they both had a similar damping response.

As will be discussed in the next section, the damping response from G22 can be viewed in Fig. 9; it provided the 3rd most substantial positive damping torque component after G7 and G9, which were already online. Throughout the VLFO, other generators' set points were also changed but this had little to no affect on the damping ratio. The change in generator set points does not appear to coincide with changes in the damping ratio. The control interventions that restored positively damped conditions were skilfully executed by the system operator to return the system to positively damped conditions.

D. DEF Analysis

Fig. 9 shows a moving window analysis of the event using DEF; changes in generator damping before, during and after the event are presented. The DEF integral gradient does become steeper, coinciding with an increase in VLF mode magnitude from window 1 to window 3.

During the ambient conditions in Fig. 9, window 1 G7 and G9 provide a strong positive damping torque component, keeping the magnitude of the VLF mode less than 20 mHz. Although six units are causing negative damping, the positive damping from other units outweighs their influence.

Window 2 covers an ambient period, like window 1, but the VLF amplitude has increased. The integrated DEF in window 2 demonstrates how the negative damping from G1 has increased and may be responsible for exciting other units with a negative damping coefficient by increasing the oscillation amplitude. While the negative damping from G1 is increasing and positive damping from G7 and G9, overall damping is tending into non-stable, negatively damped conditions. A real-time DEF analysis would have identified the approach of a VLFO tipping point and identified the generators responsible. Analysis of oscillation amplitude pre-event does not warrant any alarm, as a mode amplitude

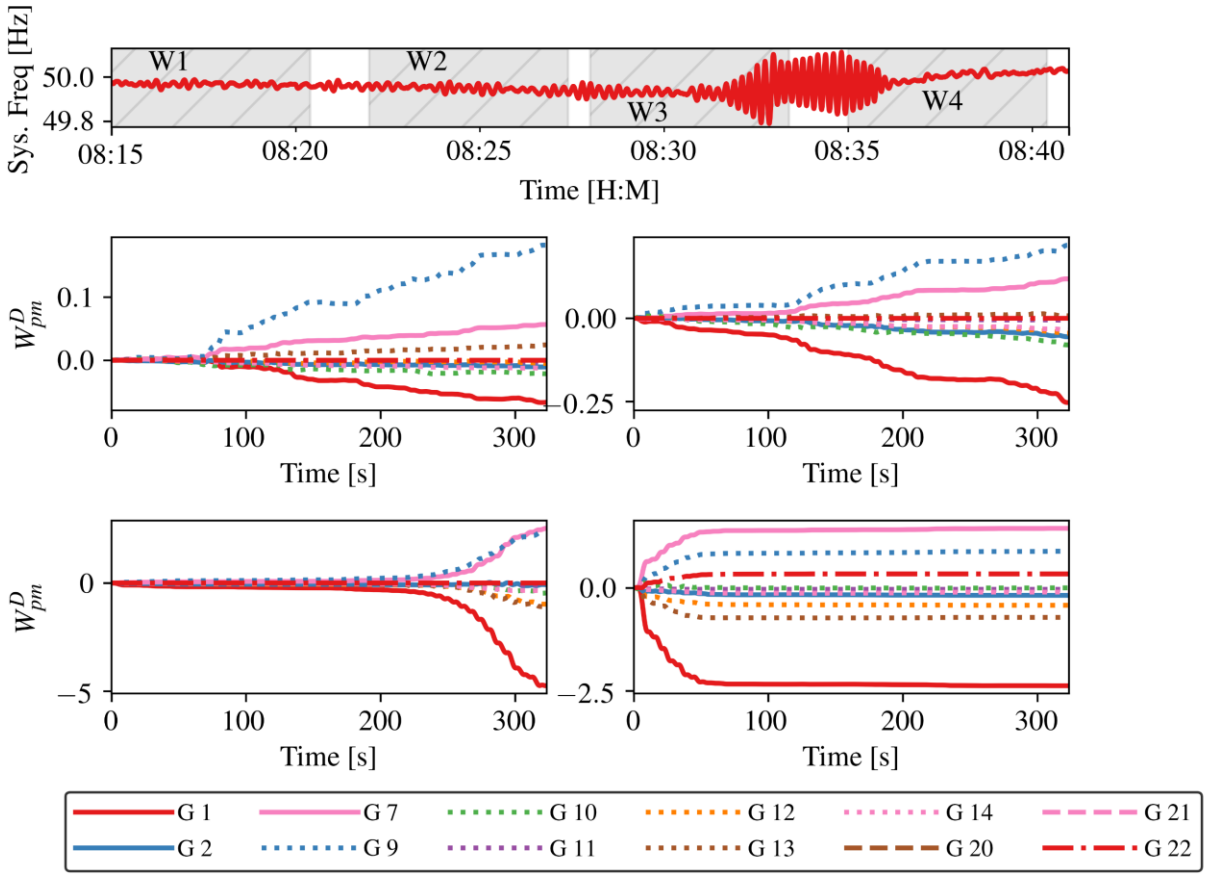

Fig 9: DEF analysis of 300 mHz Event (a) System Frequency plot (top plot) (b) DEF of window 1 (top left) (c) DEF of window 2 (top right) (d) DEF of window 3(bottom left) (e) DEF of window 4 (bottom right)

of 30 mHz does not significantly exceed normal operating parameters.

Window 3 shows the event's onset; G1 appears to have been self-excited, as shown by the DEF analysis. There is a clear divergence in window 3 where G1 is driving the oscillation on the system. G7 and G9 still maintain significant positive damping, but the other generators' negative damping outweighs their contribution. The operation of G1 appears to cause further negative damping from units that previously were providing weak or negative damping torque.

Window 4 showed DEF analysis when the system returned to positive damping. As mentioned in the previous Section III.B, two units were synchronised, one of which was G22. Although the positive damping responses from G22 and the other synchronised unit were significantly less than G7 and G9, it was enough to return the system to positively damped conditions.

E. VLFOs Active Power Magnitude

Active power magnitude is often used for oscillation source identification. Although active power magnitude may signify the source for the most significant oscillations, it is still not the best practice. It fails to distinguish between negatively and positively damping units. Active power magnitude also does not correlate with the mode of power and frequency oscillations.

Active power analysis is presented in Fig 10; while G1 stands out as delivering most of the exciting active power, it does not distinguish beneficial units from detrimental units. If the control decision was made to switch off the governor at G1, then the oscillation may have been resolved immediately, as simulated in Section III and Fig. 5b. If a decision was made to turn off the governor at G7 or G9, it could have resulted in a further decrease of the damping ratio. Active power analysis indicates that G13 may have played a role in triggering the oscillation. From a direct observation of the PMU event data and DEF analysis, it is determined that the response from G13 was coincidental and not causal. From a longitudinal study of PMU data from this unit, an irregular power response with system frequency has been noted; it is a response that is often observed and does not track the VLF mode.

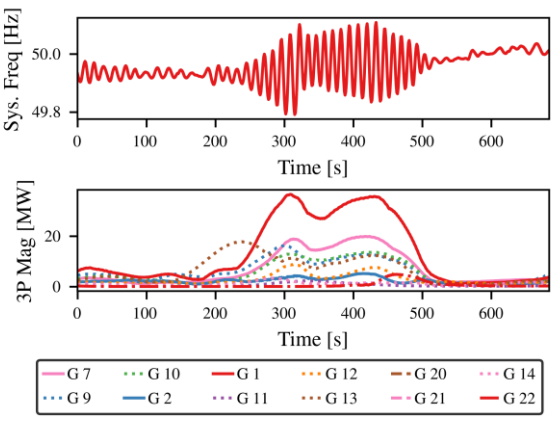

Fig 10: (a) System frequency trace (b) Oscillation magnitude extracted by CWT local maxima technique

F. Power-Frequency Linear Relationship

Governors operate with a droop characteristic with a linear relationship between active power and frequency, meaning that as system frequency increases, power output decreases. When system frequency decreases, the governor will increase power output. VLFOs can be interpreted through the governor's power-frequency relationship by analysing the divergence in this linear relationship. However, Fig 11 shows that during the VLFO event that G1 diverged from this linear relationship and has a hysteresis feature within the governor droop curve. As expected from the DEF analysis, G7 and G9 maintain a consistent linear relationship damping the VLFO.

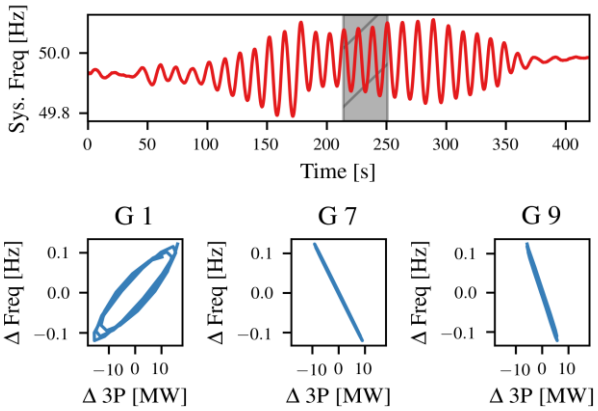

Fig 11: (a) System frequency trace (b) Active power and frequency relationship

V. Conclusions

VLFOs threaten power system security and increase wear and tear on the power system. TSOs should assess a possible "toolkit" available to pre-empt and mitigate against severe VLFOs by undergoing measurement and simulation-based studies. The main conclusions of this paper are listed as follows:

1. The simulation results show that spontaneous VLFOs can occur for differing values of generic transport delay times, creating a governor's backlash effect.
2. VLFO can be mitigated by increasing the damping ratio by synchronising generators with a positive damping governor response.
3. The most effective method of stopping a VLFO is to identify the root cause and remove it.
4. The ability to carry out this analysis in a real-time control centre is demonstrated by generator PMU data recorded during a 300 mHz VLFO on the Irish power system.
5. The methods are also used to demonstrate how the TSO restored positive damping and how they could have removed the oscillation source in a quicker time frame.

Acknowledgements

The authors would like to thank SONI/EirGrid for providing PMU data and generator metadata. The authors would also like to thank DIgSILENT PowerFactory for granting a thesis

license to continue research off-campus during COVID-19. The authors would also like to acknowledge the financial support from SPIRE 2 (Storage Platform for the Integration of Renewable Energy) project. The SPIRE 2 project is supported by the European Union's INTERREG VA Programme (Grant No. INT-VA/049), managed by the Special EU Programmes Body (SEUPB). The views and opinions expressed in this paper do not necessarily reflect those of the European Commission or the Special EU Programmes Body

REFERENCES

[1] N. Hatziargyriou, A. Rom, F. Milano, and T. Ise, "Power system frequency control : An updated review of current solutions and new challenges," vol. 194, no. December 2020, 2021.

[2] L. G. Meegahapola, S. Bu, D. P. Wadduwage, C. Y. Chung, and X. Yu, "Review on Oscillatory Stability in Power Grids with Renewable Energy Sources: Monitoring, Analysis, and Control Using Synchrophasor Technology," *IEEE Trans. Ind. Electron.*, vol. 68, no. 1, pp. 519–531, 2021.

[3] R. Xie, I. Kamwa, D. Rimorov, and A. Moeini, "Fundamental study of common mode small-signal frequency oscillations in power systems," *Int. J. Electr. Power Energy Syst.*, vol. 106, no. October 2018, pp. 201–209, 2019.

[4] Y. Shu, X. Zhou, and W. Li, "Analysis of low frequency oscillation and source location in power systems," *CSEE J. Power Energy Syst.*, vol. 4, no. 1, pp. 58–66, 2018.

[5] G. Chen *et al.*, "Optimization Strategy of Hydrogovernors for Eliminating Ultralow-Frequency Oscillations in Hydrodominant Power Systems," *IEEE J. Emerg. Sel. Top. Power Electron.*, vol. 6, no. 3, pp. 1086–1094, 2018.

[6] B. A. S. Archer, *Study and Prediction of Damping in Large Interconnected Power Systems with Applications in Monitoring Device Location, Situation Awareness and System Operation*. 2008.

[7] O. J. Arango and H. M. Sanchez, "Low Frequency Oscillations in the Colombian Power System – Identification and Remedial Actions," *Most*, pp. 1–12, 2010.

[8] B. Wall, P; Bowen, A; Geaney, C; O'Connell, "Common Mode Oscillations on the Power System of Ireland and Northern Ireland," *19th Int'l Wind Integr. Work.*, 2019.

[9] A. Wall, P; Bowen, "Analysis, Mointoring and Mitigation of the Common Mode Oscillations on the Power Systems of Ireland and Northern Ireland," in *CIGRE 2020 in Paris*, 2020, pp. 1–11.

[10] S. McGuinness, "Real-Time System Stability Analysis and Performance Monitoring using Synchrophasors," *CIGRE 2014*, 2014.

[11] S. Clark *et al.*, "VISOR Project: Initial learning from Enhanced Real Time Monitoring and Visualisation of System Dynamics in Great Britain," in *PAC World 2016, Ljubljana*, 2018, vol. PAC World, p. 36.

[12] AEMO, "Electricty Rule Change Proposal - Mandatory Frequency Response," vol. 53, no. 9, pp. 1689–1699, 2018.

[13] L. Chen, Y. Min, Y. P. Chen, and W. Hu, "Evaluation of generator damping using oscillation energy dissipation and the connection with modal analysis," *IEEE Trans. Power Syst.*, vol. 29, no. 3, pp. 1393–1402, 2014.

[14] L. Chen *et al.*, "Online emergency control to suppress frequency oscillations based on damping evaluation using dissipation energy flow," *Int. J. Electr. Power Energy Syst.*, vol. 103, no. December 2017, pp. 414–420, 2018.

[15] L. Chen, Y. Min, and W. Hu, "An energy-based method for location of power system oscillation source," *IEEE Trans. Power Syst.*, vol. 28, no. 2, pp. 828–836, 2013.

[16] M. Donnelly, D. Trudnowski, J. Colwell, J. Pierre, and L. Dosiek, "RMS-energy filter design for real-time oscillation detection," *IEEE Power Energy Soc. Gen. Meet.*, vol. 2015-Septe, pp. 1–5, 2015.

[17] D. J. Trudnowski, "Estimating electromechanical mode shape from synchrophasor measurements," *IEEE Trans. Power Syst.*, vol. 23, no. 3, pp. 1188–1195, 2008.

[18] S. Maslennikov and E. Litvinov, "ISO New England Experience in Locating the Source of Oscillations Online," *IEEE Trans. Power Syst.*, vol. 8950, no. c, pp. 1–1, 2020.

[19] F. De Marco, N. Martins, P. C. Pellanda, and A. S. E Silva, "Simulating sustained oscillations and ambient data in a large nonlinear power system model," *IEEE Power Energy Soc. Gen. Meet.*, vol. 2018-Janua, pp. 1–5, 2018.

[20] G. Jin, S. Cai, and S. Deng, "The Impact Research of Delay Time in Steam Turbine DEH on Power Grid," *J. Phys. Conf. Ser.*, vol. 1187, no. 2, 2019.

[21] L. Chen *et al.*, "Optimisation of Governor Parameters to Prevent Frequency Oscillations in Power Systems," *IEEE Trans. Power Syst.*, vol. 33, no. 4, pp. 4466–4474, 2018.

[22] R. Grondin *et al.*, "The Multi-Band PSS: A flexible Technology Designed to Meet Opening Markets," *CIGRE 2000 Paris Pap. 39-201* , no. September, 2000.

[23] G. Zhang *et al.*, "Deep Reinforcement Learning-Based Approach for Proportional Resonance Power System Stabilizer to Prevent Ultra-Low-Frequency Oscillations," *IEEE Trans. Smart Grid*, vol. 11, no. 6, pp. 5260–5272, 2020.

[24] Y. Chen, Y. Zhao, G. Geng, Q. Jiang, W. Liu, and L. Li, "Suppression Strategy of Ultra-Low Frequency Oscillation in Yunnan Power Grid with BESS," *51st North Am. Power Symp. NAPS 2019*, 2019.

[25] F. Wilches-Bernal, J. H. Chow, and J. J. Sanchez-Gasca, "A Fundamental Study of Applying Wind Turbines for Power System Frequency Control," *IEEE Trans. Power Syst.*, vol. 31, no. 2, pp. 1496–1505, 2016.

[26] IEEE Task Force on Turbine-Governor Modeling, "Dynamic Models for Turbine-Governors in Power System Studies," *Tech. Rep. PES-TR1*, pp. 1–117, 2013.

[27] P. Wang, B. Li, J. Zhao, T. Liu, Q. Jiang, and G. Chen, "The Mechanism of Ultra-Low Frequency Oscillations With the Same Mode Shapes," *IEEE Access*, vol. 8, pp. 198047–198057, 2020.

[28] D. Rimorov, I. Kamwa, and G. Joos, "Quasi-Steady-State Approach for Analysis of Frequency Oscillations and Damping Controller Design," *IEEE Trans. Power Syst.*, vol. 31, no. 4, pp. 3212–3220, 2016.

[29] P. Tripathy, S. C. Srivastava, and S. N. Singh, "A modified TLS-ESPRIT-based method for low-frequency mode identification in power systems utilising synchrophasor measurements," *IEEE Trans. Power Syst.*, vol. 26, no. 2, pp. 719–727, 2011.

[30] Eirgrid Group, "EirGrid Grid Code." http://www.eirgridgroup.com/site-files/library/EirGrid/Grid-Code.pdf (accessed Feb. 23, 2021).

APPENDIX A: MODIFIED 2-AREA SYSTEM PARAMETERS

Synchronous Machine Model - GENROU			
$Td0'$	8	xq	1.7
$Tq0'$	0.4	$xrld$	0
$Td0''$	0.03	$xrlq$	0
$Tq0''$	0.05	xd'	0.3
H	5	xq'	0.55
D	0	xd''	0.25
xd	1.8	xq''	0.25

Governor Model - GAST			
T_1	0.45	At	1
T_2	0.4	Kt	2
T_3	2	V_{min}	0
		V_{max}	1

Generators						
Name	G1	G2	G3	G4	G5	G6
MVA	900	900	900	900	100	100
R	0.03	0.05	0.05	0.05	0.03	0.03
Dead band	0	0	0	0	1	1
3P [MW]	690	700	516	700	10	10
3Q [MVAr]	200.5	92.2	59.15	13.48	10	10

Loads			
	Load A	Load B	Load C
3P [MW]	1190	1463	0.01
3Q [MVAr]	100	100	0